



Article

Chiral Thioxanthenes as Modulators of P-glycoprotein: Synthesis and Enantioselectivity Studies

Ana Lopes ¹, Eva Martins ², Renata Silva ^{2,*}, Madalena M. M. Pinto ^{1,3} , Fernando Remião ², Emília Sousa ^{1,3,*}  and Carla Fernandes ^{1,3}

¹ Laboratory of Organic and Pharmaceutical Chemistry, Department of Chemical Sciences, Faculty of Pharmacy, University of Porto, Rua Jorge Viterbo Ferreira 228, 4050-313 Porto, Portugal; up201402466@ff.up.pt (A.L.); madalena@ff.up.pt (M.M.M.P.); cfernandes@ff.up.pt (C.F.)

² REQUIMTE, Laboratory of Toxicology, Department of Biological Sciences, FFUP – Faculty of Pharmacy, University of Porto, Rua de Jorge Viterbo Ferreira, 228, 4050-313 Porto, Portugal; up201204736@fc.up.pt (E.M.); remiao@ff.up.pt (F.R.)

³ Interdisciplinary Centre of Marine and Environmental Research, University of Porto, Terminal de Cruzeiros do Porto de Leixões, Av. General Norton de Matos s/n, 4450-208 Matosinhos, Portugal

* Correspondence: rsilva@ff.up.pt (R.S.); esousa@ff.up.pt (E.S.); Tel.: +351-22-042-8689 (E.S.)

Received: 7 February 2018; Accepted: 7 March 2018; Published: 10 March 2018

Abstract: Recently, thioxanthone derivatives were found to protect cells against toxic P-glycoprotein (P-gp) substrates, acting as potent inducers/activators of this efflux pump. The study of new P-gp chiral modulators produced from thioxanthone derivatives could clarify the enantioselectivity of this ABC transporter towards this new class of modulators. The aim of this study was to evaluate the P-gp modulatory ability of four enantiomeric pairs of new synthesized chiral aminated thioxanthenes (ATxs) 1–8, studying the influence of the stereochemistry on P-gp induction/ activation in cultured Caco-2 cells. The data displayed that all the tested compounds (at 20 μ M) significantly decreased the intracellular accumulation of a P-gp fluorescent substrate (rhodamine 123) when incubated simultaneously for 60 min, demonstrating an increased activity of the efflux, when compared to control cells. Additionally, all of them except ATx 3 (+), caused similar results when the accumulation of the P-gp fluorescent substrate was evaluated after pre-incubating cells with the test compounds for 24 h, significantly reducing the rhodamine 123 intracellular accumulation as a result of a significant increase in P-gp activity. However, ATx 2 (–) was the only derivative that, after 24 h of incubation, significantly increased P-gp expression. These results demonstrated a significantly increased P-gp activity, even without an increase in P-gp expression. Therefore, ATxs 1–8 were shown to behave as P-gp activators. Furthermore, no significant differences were detected in the activity of the protein when comparing the enantiomeric pairs. Nevertheless, ATx 2 (–) modulates P-gp expression differently from its enantiomer, ATx 1 (+). These results disclosed new activators and inducers of P-gp and highlight the existence of enantioselectivity in the induction mechanism.

Keywords: P-glycoprotein; thioxanthenes; enantioselectivity; expression; activation

1. Introduction

P-glycoprotein (P-gp) is the best characterized efflux transporter belonging to the superfamily of ATP-binding cassette (ABC) transporters [1–4]. The structure of P-gp complies with the prototype characteristics described for the ABC transporters, being a polypeptide made up of two homologous halves that arise from a gene duplication event [5–7]. Each half contains a transmembrane domain

(TMD), formed of six membrane-spanning α helices (TMHs), and a nucleotide binding domain (NBD), located at the cytoplasmic side of the membrane [4,8–10]. This 170 kDa protein, also known as ABCB1, is encoded in humans by the multidrug resistance (MDR) genes *MDR1* (*ABCB1*) and *MDR3* (*ABCB4*), being the multidrug resistance (MDR) phenotype associated with the ABCB1 isoform. Also, the term P-gp refers, usually, to the ABCB1 isoform [4,5,10].

P-gp is broadly expressed in normal tissues, as well as in brain, liver, small intestine, kidney and lung [2,11,12]. Using the energy from ATP hydrolysis, the P-gp promotes the outward transport of a large range of structurally unconnected compounds [4,7,13]. Therefore, it plays important physiological functions, being its primary function to protect the cells against toxic xenobiotics and endogenous metabolites [1,7]. Furthermore, this efflux pump plays a key role in the absorption, elimination, disposition and toxicity of a wide range of compounds, both endobiotics and xenobiotics, since it is responsible for their transport across cell membranes [14,15]. Additionally, it is important to maintain the barrier function of numerous tissues, such as the small intestine, blood–brain barrier and placenta [4,7,9,14,16]. Considering that many drugs used in clinical treatments are substrates of P-gp, their pharmacokinetic processes and, consequently, their effectiveness, can be greatly affected by the level of expression and functionality of this pump [4,7,16,17]. When a drug that is a P-gp substrate is co-administrated with another drug, a P-gp inducer, activator or inhibitor, the pharmacokinetics and bioavailability of the P-gp substrate may be substantially altered [16,18].

Over the years, P-gp modulation has been seen like a vital area in drug development [4,9,11,19–22]. In fact, due to the P-gp role in MDR, the first studies on this efflux pump were mostly focused on its inhibition as a therapeutic option to circumvent MDR in chemotherapy [3,8,11,22,23]. Since the degree of MDR is strongly correlated with changes in drug permeability, it is largely related to both P-gp expression and activity [21,24]. However, more recent insights showed that P-gp inhibitors can be also helpful to modulate the general pharmacokinetic behavior of drugs in the organism, revealing special importance in case of central nervous system (CNS) active drugs, to allow increasing drugs brain penetration [19,23,25]. Consequently, over the years, several studies were developed in order to discover potent and safe P-gp inhibitors, and to better understand their mechanisms of inhibition [3,23,25–29]. Furthermore, some recent studies have also focused on the induction/activation of this pump, and the use of such inducers/activators to avoid the toxicity mediated by substrates of P-gp has been proposed as a potential antidotal pathway [30–33]. Accordingly, the modulation of P-gp can be applied not only in drug discovery but also in drug development, to overcome the limitations of some drugs in clinical use due their interaction with P-gp, which affects their clinical effectiveness [4,13,14,29,34].

A group of studied compounds that interact with P-gp activity is the thioxanthenes, synthetic S-heterocycle compounds with a dibenzo- γ -thiopyrone scaffold. The biological interest in this class of compounds started with lucanthone, firstly introduced as an antischistosomal drug [35,36]. Over the years, diverse biological activities of thioxanthone derivatives have been described, such as P-gp modulation [21,30,37], topoisomerase inhibition [38,39], antitumor [40–46], and antimicrobial properties [40–43], among others [47–49]. A large amount of studies concerning P-gp modulation by thioxanthenes was focused on their ability to act both as P-gp inhibitors and as antitumor agents [11,13,23,25,50,51]. In these studies, some P-gp activators/inducers were disclosed [25]. Indeed, using a Caco-2 cells in vitro model, some thioxanthone derivatives were studied with the aim of evaluate their potential to increase the expression and/or activity of P-gp, and their potential protective effects in Caco-2 cells to fight the toxicity induced by paraquat (PQ) [30]. PQ is an extremely toxic herbicide that is a P-gp substrate, and was used as a model in order to develop new antidotes using this efficient antidotal pathway [30,32,33,52].

There are studies describing that P-gp can interact in a different way with enantiomers [53]. When chiral drugs modulate P-gp, one enantiomer can increase the activity of P-gp while the other enantiomer can inhibit the activity of the pump [24,54]. An example of this type of enantioselectivity was observed

for mefloquine, a drug used in the prevention and treatment of malaria: (1*R*,12*S*)-(+)-mefloquine presents a much higher human brain penetration than (1*S*,12*R*)-(–)-mefloquine [55].

Herein, we investigated the potential modulatory effect on P-gp activity and expression of four newly synthesized pairs of enantiomers of aminated thioxanthenes (ATxs 1–8, Figure 1), to clarify the enantioselectivity of this efflux pump towards the ABC transporters class. Moreover, although some examples of biological enantioselectivity were reported in the literature for structurally related xanthenes [56–58], for thioxanthenes, and specifically for P-gp modulation, data is presented here for the first time.

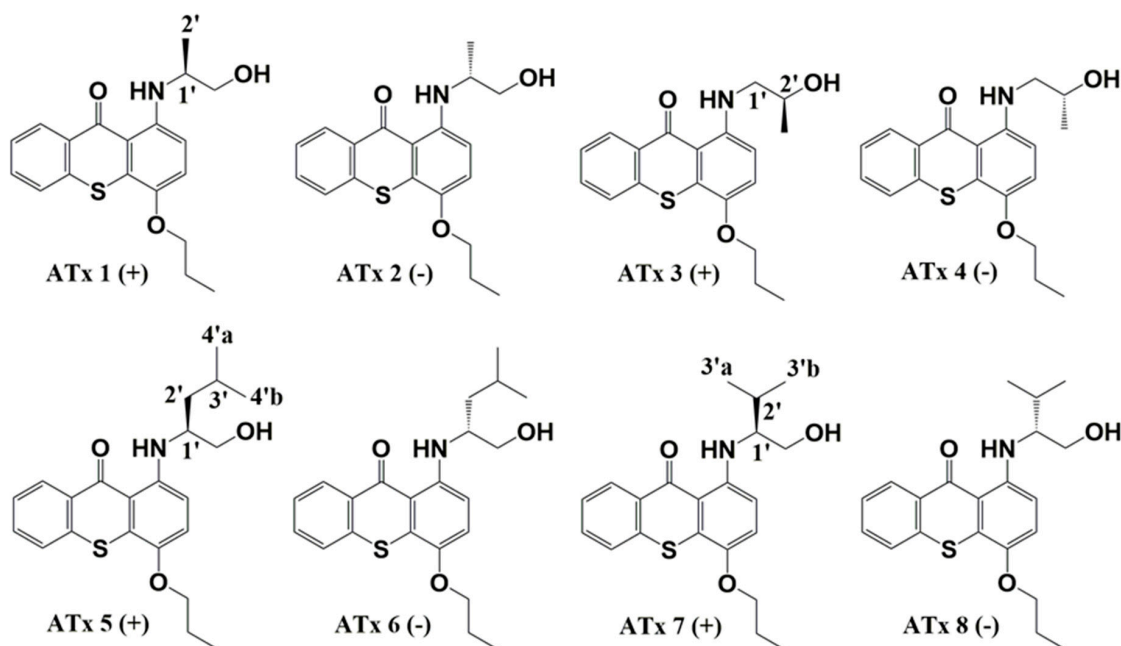
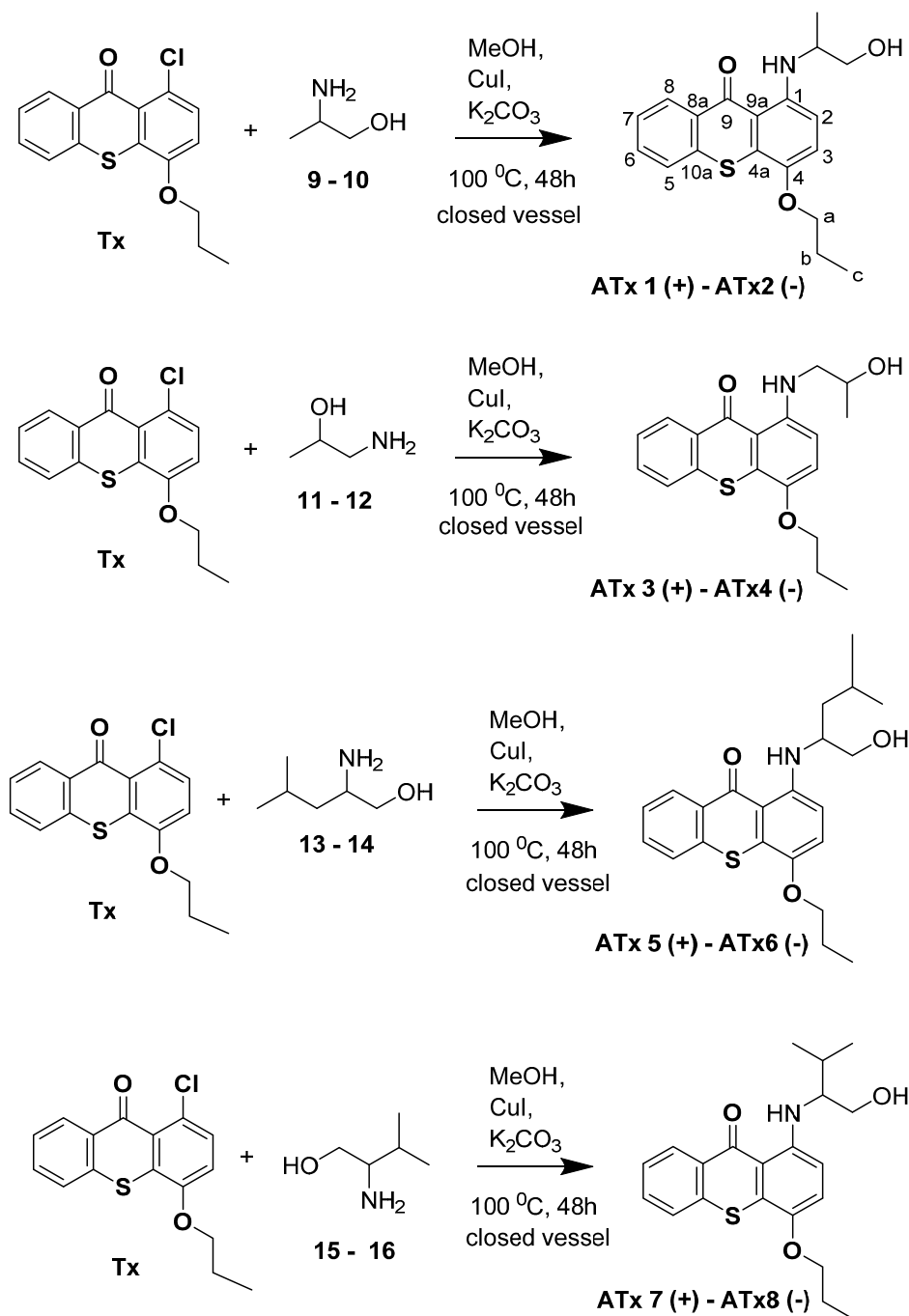


Figure 1. Structures of the studied chiral aminated thioxanthenes, ATxs 1–8.

2. Results

2.1. Synthesis of Thioxanthenes

The new chiral ATxs 1–8 were synthesized by copper-catalyzed Ullmann cross-coupling reactions between the thioxanthone derivative 1-chloro-4-propoxy-9*H*-thioxanthen-9-one (Tx) and eight enantiomerically pure amino alcohols 9–16 in alkaline medium (Scheme 1). The amino alcohols selected for this study fitted on the pharmacophore model previously built for P-gp activators and their design was based on a hit compound found as a P-gp activator/inducer, 1-[(3-hydroxypropyl)amino]-4-propoxy-9*H*-thioxanthen-9-one, a thioxanthone with an amino alcohol chain at position 1 [30]. Therefore, we decided to modify this amino alcohol chain introducing also a stereogenic center to explore the influence of chirality in this class of derivatives.



Scheme 1. Reaction conditions for the synthesis of chiral thioxanthenes 1–8 (ATxs 1–8).

Initial investigations of the catalyst to be used in the Ullman asymmetric reactions revealed copper iodide as a more efficient catalyst when compared to copper oxide used previously in the synthesis of aminated thioxanthenes [30].

The purity of each synthesized chiral thioxanthone was determined by high performance liquid chromatography with diode-array detection (HPLC–DAD) analysis. All tested compounds presented a purity of at least 95%. Their enantiomeric purity was also measured by chiral HPLC using an amylose-derived column under normal-phase or polar organic mode, achieving enantiomeric excess (e.e.) values higher than 99%, as exemplified in Figure 2 for the enantiomeric pair ATx 1 (+) and ATx 2 (–).

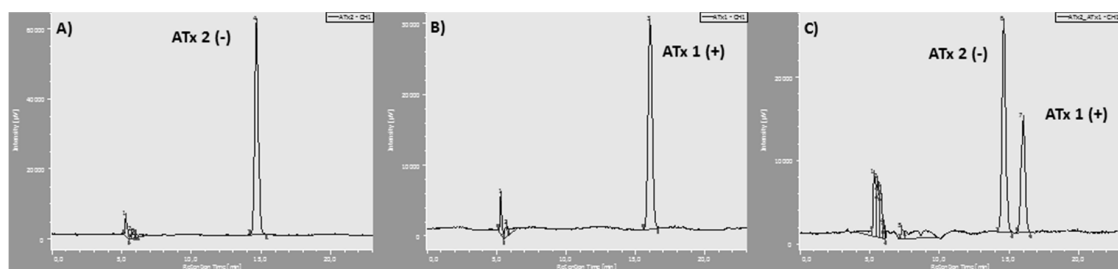


Figure 2. Chromatograms of the investigated compounds (A) (*R*)-1-((1-hydroxypropan-2-yl)amino)-4-propoxy-9*H*-thioxanthen-9-one (ATx 2 (-)), (B) (*S*)-1-((1-hydroxypropan-2-yl)amino)-4-propoxy-9*H*-thioxanthen-9-one (ATx 1 (+)), (C) (*S,R*)-1-((1-hydroxypropan-2-yl)amino)-4-propoxy-9*H*-thioxanthen-9-one (mixture of ATx 1 (+) and ATx 2 (-)) on Lux[®] 5 μ m amylose-1 at 0.5 mL/min⁻¹; *n*-hexane:ethanol (70:30 *v/v*), 0.5 mL/min, λ_{\max} 254 nm.

The structure elucidation of all new thioxanthonic derivatives (ATxs 1–8) was established by spectroscopic methods: infrared (IR), ¹H- and ¹³C-nuclear magnetic resonance (NMR), and bidimensional heteronuclear single quantum correlation (HSQC) and heteronuclear multiple bond correlation (HMBC). Since these determinations were performed in achiral environments, no significant differences were noted for each pair of enantiomers obtained, as expected. The ¹³C-NMR assignments were made by HSQC and HMBC experiments and by comparison with assignments of similar molecules [25,58]. The HMBC data were important to deduce the chemical shifts of quaternary carbons and confirm the C–N coupling product.

2.2. Chiral Thioxanthonic Cytotoxicity Assays

Chiral ATxs 1–8 cytotoxicity was evaluated by the neutral red (NR) uptake assay, in order to select a noncytotoxic working concentration to be used in the subsequent studies that aim to evaluate their potential to induce and/or activate P-gp. After 24 h of incubation, significant cytotoxicity was observed for the 50 μ M concentration of chiral ATxs 1 (+), 2 (-), 6 (-), 7 (+) and 8 (-) (Figure 3). For ATxs 3 (+), 4 (-), and 5 (+) no significant cytotoxicity was observed after 24 h of incubation within the tested concentration range (0–50 μ M). Therefore, chiral thioxanthonic effect on P-gp expression and activity was further evaluated using a noncytotoxic concentration of 20 μ M.

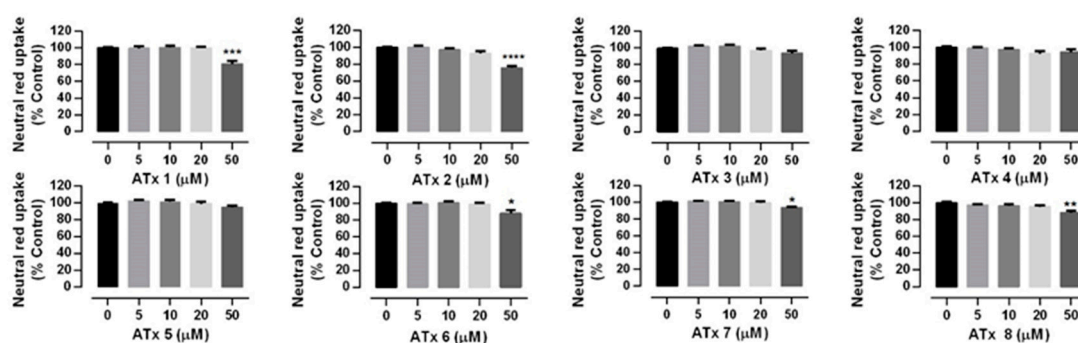


Figure 3. Chiral thioxanthonic ATxs 1–8 (0–50 μ M) cytotoxicity in Caco-2 cells evaluated by the Neutral Red uptake assay, 24 h after exposure. Results are presented as mean \pm standard error mean (SEM) from at least 5 independent experiments (performed in triplicate). Statistical comparisons were estimated using the nonparametric method of Kruskal–Wallis (one-way ANOVA on ranks), followed by the Dunn's multiple comparisons post hoc test (* $p < 0.05$; ** $p < 0.01$; *** $p < 0.001$; **** $p < 0.0001$ vs. control (0 μ M)).

2.3. Flow Cytometry Analysis of P-gp Expression

The ability of the tested chiral ATx's 1–8 to induce P-gp expression in Caco-2 cells was evaluated by flow cytometry, using a P-gp monoclonal antibody (UIC2) conjugated with phycoerythrin (PE), 24 h after exposure. As shown in Figure 4, ATx 2 (–) significantly increased P-gp expression by 36%, when compared to control cells. For the other tested chiral thioxanthenes, no significant effect on P-gp expression was observed after 24 h of incubation. Furthermore, significant differences were detected in the P-gp induction mediated by the enantiomeric pair ATx 1 (+) : ATx 2 (–), demonstrating an enantioselectivity for P-gp induction.

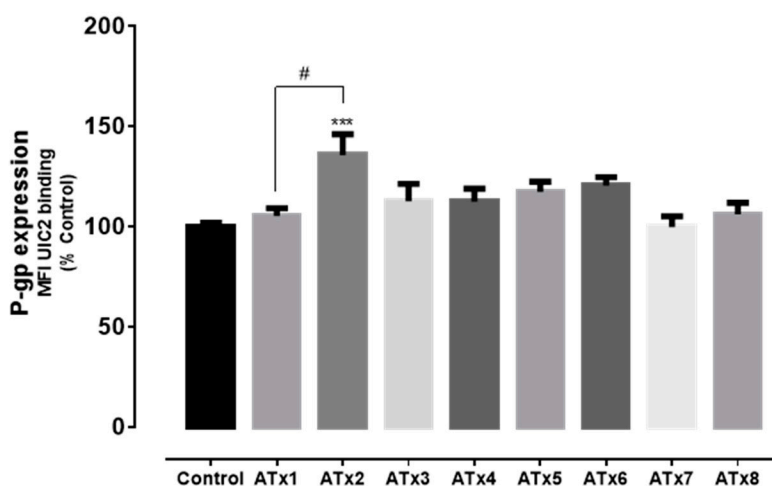


Figure 4. Flow cytometry analysis of P-gp expression levels in Caco-2 cells exposed to ATxs 1–8 (20 μ M) for 24 h. Results are presented as mean \pm standard error mean (SEM) from 5 independent experiments (performed in duplicate). Statistical comparisons were made using One-way ANOVA, followed by Tukey's multiple comparisons test (***) $p < 0.001$ vs. control (0 μ M); # $p < 0.05$ for ATx 1 (+) vs. ATx 2 (–)).

2.4. Evaluation of P-gp Transport Activity

The P-gp transport activity was evaluated by flow cytometry using rhodamine (RHO) 123, a P-gp fluorescent substrate [25,31]. Two different approaches were used. In the first approach, RHO 123 accumulation was evaluated in the presence of the tested chiral ATxs 1–8 (20 μ M) during the RHO 123 accumulation phase that lasted 60 min, in order to evaluate the potential immediate effects of the tested compounds on P-gp activity as a result of a direct activation of the pump. P-gp activity was evaluated through the ratio between the mean intracellular RHO 123 fluorescence intensity (MFI) obtained under P-gp inhibition (IA) and the MFI observed in normal conditions (NA, in the absence of P-gp inhibition) (Equation (1)), and expressed as percentage of control cells (0 μ M chiral ATxs).

A higher P-gp activity, originate a higher ratio from a smaller MFI NA, as the dye is being pumped out of the cells during the accumulation phase. As observed in Figure 5, all the tested compounds 1–8 induced a significant increase in P-gp activity, when compared to control cells (P-gp activity significantly increased to 121, 132, 121, 114, 124, 127, 131 and 121% for ATx 1 (+), ATx 2 (–), ATx 3 (+), ATx 4 (–), ATx 5 (+), ATx 6 (–), ATx 7 (+) and ATx 8 (–), respectively). From the tested compounds, ATx 2 (–) and ATx 7 (+) were the most efficient P-gp activators, as exposed by the increased RHO 123 accumulation ratio, that resulted from an decreased RHO 123 intracellular accumulation.

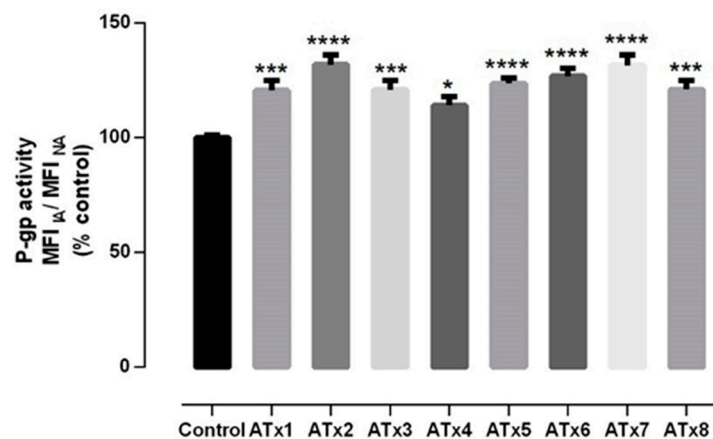


Figure 5. P-gp activity evaluated through the RHO 123 accumulation in the presence of chiral ATxs 1–8 (20 μ M) during the RHO 123 accumulation phase. Results are presented as mean \pm SEM from five independent experiments (performed in triplicate). Statistical comparisons were estimated using One-way ANOVA, followed by Tukey's multiple comparisons test (* $p < 0.05$; *** $p < 0.001$; **** $p < 0.0001$ vs. control (0 μ M)).

In the second protocol, RHO 123 accumulation was evaluated in Caco-2 cells pre-exposed to the tested chiral thioxanthenes (20 μ M) for 24 h. With this second approach, it was possible to assess whether the increased P-gp expression induced by the chiral thioxanthenes is accompanied by the matching increases in P-gp activity, given that an increased protein expression does not always mean an increased transport activity [31,59–61]. The obtained results (Figure 6) demonstrated a significant increase in P-gp activity for seven of the tested compounds, namely ATx 1 (+), ATx 2 (–) ATx 4 (–), ATx 5 (+), ATx 6 (–), ATx 7 (+) and ATx 8 (–). In fact, P-gp activity increased to 163, 167, 147, 176, 169, 167 and 165% for ATx 1 (+), ATx 2 (–), ATx 4 (–), ATx 5 (+), ATx 6 (–), ATx 7 (+) and ATx 8 (–), respectively. For ATx 3 (+), no significant increase in P-gp activity was observed when compared to control cells (P-gp activity increased only to 115%).

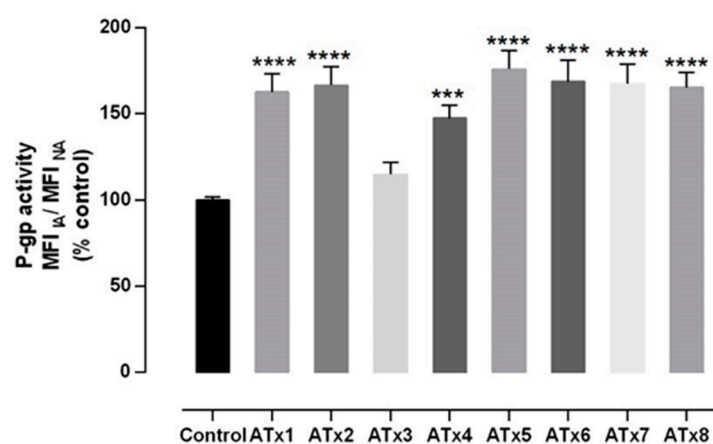


Figure 6. P-gp activity evaluated through the RHO 123 accumulation in Caco-2 cells exposed to chiral thioxanthenes (20 μ M) for 24 h. Results are presented as mean \pm SEM from four independent experiments (performed in duplicate). Statistical comparisons were estimated using One-way ANOVA, followed by Tukey's multiple comparisons test (*** $p < 0.001$; **** $p < 0.0001$ vs. control (0 μ M)).

2.5. Determination of ATPase Activity

The effect of chiral ATxs 1–8 on the ATPase activity of P-gp was evaluated through the detection and quantification of the unmetabolized ATP, as a luciferase-generated luminescent signal, in human

P-gp-enriched membranes. P-gp-dependent decreases in luminescence reflect ATP consumption by P-gp and, consequently, a decrease in the obtained signal reflects the presence of a compound that stimulates P-gp ATPase activity.

In the present study, Na_3VO_4 (sodium orthovanadate) was used as a selective P-gp inhibitor and, thus, samples treated with Na_3VO_4 have no P-gp ATPase activity. Consequently, the difference in luminescent signal between Na_3VO_4 -treated samples and untreated samples ($\Delta\text{RLU}_{\text{basal}}$) reflects the basal P-gp ATPase activity, whereas the difference in luminescent signal between Na_3VO_4 -treated samples and samples treated with the test compound (TC) ($\Delta\text{RLU}_{\text{TC}}$) represents the P-gp ATPase activity in the presence of the test compound. Therefore, the test compound can be a stimulator of P-gp ATPase activity if $\Delta\text{RLU}_{\text{TC}} > \Delta\text{RLU}_{\text{basal}}$; can be an inhibitor of P-gp ATPase activity if $\Delta\text{RLU}_{\text{TC}} < \Delta\text{RLU}_{\text{basal}}$; or can have no effect on P-gp ATPase activity if $\Delta\text{RLU}_{\text{TC}} = \Delta\text{RLU}_{\text{basal}}$. Verapamil (Ver) was used in the present assay as a positive control since it is a substrate for P-gp-mediated transport, thus stimulating P-gp ATPase activity. The results for the eight tested compounds and Ver are shown in Figure 7, as well as the basal P-gp ATPase activity. None of the tested compounds (ATx's 1–8) caused a significant change in the ΔRLU when comparing to the basal P-gp ATPase activity, demonstrating not being substrates for this efflux pump.

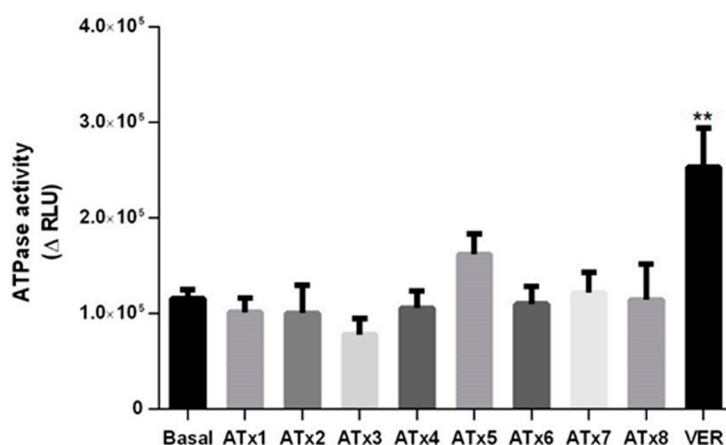


Figure 7. P-gp ATPase activity in the presence of chiral ATxs 1–8. Results are expressed as mean \pm SEM from three independent experiments (performed in triplicate). Statistical comparisons were estimated using One-way ANOVA, followed by Tukey's multiple comparisons test (** $p < 0.01$ vs. basal P-gp ATPase activity).

3. Discussion

All chiral aminated thioxanthenes, ATxs 1–8, were synthesized in enantiomerically pure form in order to study the effect of the stereochemistry in P-gp modulation. The reaction conditions used in the Ullmann cross-coupling reaction between a suitable functionalized thioxanthone with enantiomerically pure building blocks allowed a successful synthesis of the desired chiral thioxanthenes in moderate yields. The purification process applied allowed us to obtain the desired compounds (ATxs 1–8) with a purity of at least 95% and e.e. higher than 99%. Sufficient amounts were obtained to proceed with the evaluation of the biological activity. Structure elucidation of ATxs 1–8 was confirmed by spectroscopic methods. The e.e. values obtained by chiral HPLC evaluation as well as the absolute values of specific rotation confirmed that no racemization occurred under these reaction conditions.

Caco-2 cells express P-gp at levels similar to those found in normal human jejunum [62] and they were already validated as a suitable in vitro model for the evaluation of P-gp modulation [30–32,52]. Previous studies demonstrated that newly synthesized thioxanthone derivatives significantly increased both P-gp expression and activity in Caco-2 cells, 24 h after exposure, being the first report on the ability of such compounds to act as P-gp inducers [30]. Moreover, although it is known that increases in protein expression may not necessarily result in proportional increases in the pump activity [31,60,61],

for these compounds, the detected increases in the cell surface P-gp expression (since the UIC2 monoclonal antibody used in the experiments recognizes an external P-gp epitope) were accompanied by similar increases in its transport activity [30]. An important aspect to note among the obtained data was the ability of all the tested chiral thioxanthenes to rapidly and significantly increase P-gp activity, without interfering with its expression, an effect compatible with a P-gp activation phenomenon [30].

In the present study, ATxs 1–8 also demonstrated to be P-gp activators since they were able to significantly increase P-gp transport function without interfering with the protein expression levels, as demonstrated by the data obtained in the RHO 123 accumulation assay performed in the presence of the chiral thioxanthenes during a short 60 min accumulation phase. Concerning their structure, a chiral center further away of the thioxanthone moiety seems to prejudice the P-gp activation effect in this series of compounds. The RHO 123 accumulation evaluated using this protocol does not reflect a possible contribution of an increased P-gp expression in the increased activity due to the short duration of the contact between the chiral thioxanthenes and the cells during the RHO 123 accumulation phase.

Furthermore, and contrarily to what was observed in the previously mentioned study [30], in the present work, the data obtained for the eight tested compounds demonstrated that, although only chiral ATx 2 (–) caused a significant increase in P-gp expression 24 h after exposure, all the tested compounds significantly increased P-gp activity when RHO 123 accumulation was evaluated 24 h after exposure, except for ATx 3 (+). In fact, and as previously mentioned, it is known that increases in protein expression may not necessarily result in proportional increases in pump activity, and that increases in activity can be observed independently of the level of expression. Indeed, although chiral ATxs 1 (+), 4 (–), 5 (+), 6 (–), 7 (+) and 8 (–) were not able to significantly increase P-gp expression 24 h after exposure, a significant increased P-gp activity was observed in Caco-2 cells pre-exposed to the tested compounds for this incubation period. Therefore, since these compounds demonstrated to be P-gp activators (as demonstrated by the significant differences observed in the RHO 123 accumulation assay performed with the compounds present only during the short RHO 123 accumulation phase), the observed increases in the pump activity must result from a direct pump activation, instead of an increased P-gp expression. The observed P-gp activation may be caused by the compound that remains intracellularly, once the cells are pre-exposed to the tested compounds for 24 h, and washed (to remove the tested compounds) prior to the evaluation of P-gp activity. In what concerns to P-gp ATPase activity, in contrast to previous findings [30], no significant differences were observed between the P-gp ATPase activity in the presence of the investigated thioxanthenes and the basal P-gp ATPase activity. These ATxs 1–8 with a chiral center in the α -position of the aniline moiety seem not to affect the P-gp ATPase activity, and are unlikely to be substrates for P-gp-mediated transport, since P-gp substrates, like verapamil, typically stimulate its ATPase activity.

Although, some examples of enantioselective modulation of P-gp with other class of compounds have been described [54,55,63,64], no studies were reported focusing the enantioselectivity of chiral thioxanthenes in modulating P-gp. Comparing the results obtained for the studied enantiomeric pairs (ATxs 1 (+) and 2 (–), ATxs 3 (+) and 4 (–), ATxs 5 (+) and 6 (–), and ATxs 7 (+) and 8 (–)), no significant differences were observed in P-gp activity. In contrast, for the P-gp induction effect for the chiral pair ATxs 1 (+) and 2 (–), significant differences were found. Noteworthy, a chiral center with *R* configuration closer to the thioxanthone moiety and with less hindered substituents seems to be critical for the induction effect in this series of compounds. This result highlights the existence of enantioselectivity in what concerns to induction mechanism, which is not a consequence of a direct interaction with P-gp. Previously, a similar behavior was described for the H1 anti-histaminic cetirizine, which was also ascribed to effects on P-gp expression [54]; the (*R*)-cetirizine upregulates P-gp expression, while (*S*)-cetirizine down-regulates it [54,65]; although, this library of compounds did not display any direct stereoselective modulation of P-gp, as previously observed for other substrates [54,55,63,64].

4. Materials and Methods

4.1. General Information

All reagents and solvents were purchased from Sigma Aldrich Co. (St. Louis, MO, USA), and no further purification was used. The amine building blocks **9–16** were (S)-(+)-amino-1-propanol (**9**), (R)-(–)-2-amino-1-propanol (**10**), (S)-(+)-1-amino-2-propanol (**11**), (R)-(–)-1-amino-2-propanol (**12**), (S)-(+)-leucinol (**13**), (R)-(–)-leucinol (**14**), (S)-(+)-valinol (**15**) and (R)-(–)-valinol (**16**). Dulbecco's modified Eagle's medium (high glucose), rhodamine 123 (RHO 123), elacridar and neutral red (NR) solution were obtained from Sigma (St. Louis, MO, USA). Reagents used in cell culture, including nonessential amino acids (NEAA), heat inactivated fetal bovine serum (FBS), 0.25% trypsin/1 mM EDTA, antibiotic (10,000 U/mL penicillin, 10,000 µg/mL streptomycin) and human transferrin (4 mg/mL) were purchased from Gibco Laboratories (Lenexa, KS, USA). P-gp monoclonal antibody (clone UIC2) conjugated with phycoerythrin (PE) was purchased from Abcam (Cambridge, UK). Flow cytometry reagents (sheath fluid, cleaning solution, decontamination solution, extended flow cell clean) were purchased from BD Bioscience (San Jose, California, USA). The Pgp-Glo™ assay system was purchased from Promega Corporation (Madison, WI, USA). All the reagents used were of analytical grade or of the highest grade available. Reactions were performed in a muffle for 48 h at 100 °C.

Flash column chromatography using silica gel 60 (0.040–0.063 mm, Merck, Darmstadt, Germany), flash cartridge chromatography (GraceResolv®, Grace Company, Deerfield, IL, USA), and Discovery® DSC-SCX SPE cationic exchange cartridge (Grace Company, Deerfield, IL, USA) were used in the purification of the synthesized compounds. Melting points (m.p.) were obtained in a Köfler microscope (Santiago, Ostrava, Czech Republic) and are uncorrected. Infrared (IR) spectra were obtained in KBr microplates on a Nicolet iS10 Fourier transform infrared spectroscopy spectrometer from Thermo Scientific (Waltham, MA, USA) with a Smart OMNI-Transmission accessory (Software OMNIC 8.3, Waltham, MA, USA). Optical rotation measurements were carried out on a Polartronic Universal polarimeter (Bellingham + Stanley Ltd., Tunbridge Wells, Kent, UK). NMR spectra were recorded at the University of Aveiro, Department of Chemistry in CDCl₃ (Deutero GmbH, Ely, UK) at room temperature on an Avance 300 spectrometer (300.13 MHz for ¹H and 75.47 MHz for ¹³C, Bruker, Bruker Biosciences Corporation, Billerica, MA, USA). ¹³C-NMR assignments were made by bidimensional HSQC and HMBC experiments (long-range C, H coupling constants were optimized to 7 and 1 Hz) or by comparison with the assignments of similar molecules.

HPLC analysis were performed on a Finnigan Surveyor (Thermo Electron Corporation, Cleveland, OH, USA) equipped with an autosampler (AutoSampler Plus) and a TSP UV8000LP diode array detector (Thermo Electron Corporation). The treatment of the chromatographic data was performed using the Xcalibur® 2.0 SUR1 software (Thermo Electron Corporation). For purity evaluation, the chromatographic separation was carried out on 250 × 4.6 mm i.d. FortisBIO C18 column (5 µm) with the mobile phase methanol:water:trimethylamine (80:20:0.5 v/v/v). The mobile phase was prepared in a volume/volume relation and degassed in an ultrasonic bath for 15 min before use. The flow rate was 1.0 mL/min. Aliquots of 20 µL of each synthesized chiral thioxanthone (ATxs **1–8**) at the concentration of 20 µg/mL were injected. For e.e. evaluation, the chromatographic column used was a 250 × 4.6 mm i.d. Lux® Amylose-1 (5 µm) from Phenomenex (Torrance, CA, USA). Analyses were performed in isocratic mode, at 22 ± 2 °C, in normal phase, using a mixture of *n*-hexane:ethanol (70:30 v/v) as mobile phase, or polar organic elution mode, using methanol or acetonitrile as mobile phase. The flow rate used was 0.5 mL/min. The UV detection was set at a wavelength of 254 nm and 20 µL of sample were injected in triplicate. The e.e. was determined by the relative percentages of the peak areas according to [e.e. (%) = 100 × ([R] – [S])/([R] + [S]) or 100 × ([S] – [R])/([S] + [R])], where [S] and [R] are the peak areas of each enantiomer.

4.2. Synthesis of Chiral Thioxanthenes (ATxs 1–8)

1-Chloro-4-propoxy-9H-thioxanthen-9-one (Tx, 450 mg, 1.48 mmol) and a suitable chiral amino alcohol (9–16, 1.72 mmol) were dissolved in methanol (30 mL) and CuI (0.15 mmol) and K₂CO₃ (1.92 mmol) were added. The reaction mixture was heated at 100 °C in a muffle furnace for 48 h. After the completion of the reaction, the crude material was filtrated, washed with dichloromethane, and the organic solvents were evaporated under reduced pressure. Then, the obtained solid was dissolved in 50 mL of dichloromethane and extracted with HCl 1 M (3 × 50 mL). The aqueous layer was basified with NaOH 20% and extracted with dichloromethane (3 × 100 mL). The organic layers were gathered, washed with water (3 × 50 mL), dried over anhydrous sodium sulphate and the solvent was evaporated under reduced pressure. Then, a solid phase extraction using a cation exchange cartridge Discovery[®] DSC-SCX was applied to further purify the extracted material. First, an activation of the cartridge with dichloromethane (50 mL) was performed followed by loading the cartridge with the sample (previously incorporated in silica). Then, elution was carried out with the following solvents: dichloromethane, a mixture of dichloromethane/methanol 5:5 (*v/v*), methanol 100% and NH₃ 2% in methanol. The fractions containing the chiral ATxs were gathered and the solvent was evaporated under reduced pressure. A flash column chromatography with *n*-hexane/ethyl acetate in gradient and crystallization from chloroform and petroleum ether (4:1) were also performed to obtain pure compounds.

(*S*)-1-((1-Hydroxypropan-2-yl)amino)-4-propoxy-9H-thioxanthen-9-one (ATx 1 (+)). Yield: 1.97%. m.p.: 116–118 °C (dec.); $[\alpha]_{\text{D}}^{25} +112^{\circ}$ ($c = 3.4 \times 10^{-3}$ g/mL in dichloromethane). IR (KBr) ν_{max} : 3419, 3270, 2962, 2925, 2873, 2359, 2341, 1618, 1568, 1507, 1435, 1293, 1269, 1252, 1225, 746 cm⁻¹. ¹H-NMR (300.13 MHz, CDCl₃): δ : 8.50 (1H, d, $J = 8.0$ Hz, H-8), δ : 7.56 (2H, m, H-5 and H-6), δ : 7.43 (1H, m, H-7), δ : 7.13 (1H, d, $J = 9.0$ Hz, H-3), δ : 6.85 (1H, d, $J = 9.0$ Hz, H-2), δ : 4.03 (2H, t, $J = 6.5$ Hz, H-a), δ : 3.81 (3H, m, H-1' and CH₂OH), δ : 1.90 (2H, m, H-b), δ : 1.32 (3H, d, $J = 6.2$ Hz, H-2'), δ : 1.12 (3H, t, $J = 7.4$ Hz, H-c). ¹³C-NMR (75.47 MHz, CDCl₃): δ : 183.55 (C-9), 146.50 (C-4), 144.02 (C-1), 136.85 (C-6), 131.92 (C-8a), 129.85 (C-4a), 129.24 (C-9a), 126.08 (C-8), 125.98 (C-7), 125.20 (C-5), 119.12 (C-3), 114.10 (C-10a), 109.80 (C-2), 72.48 (C-a), 65.96 (C-CH₂OH), 51.91 (C-1'), 22.66 (C-b), 16.86 (C-2'), 10.71 (C-c). e.e. > 99% (HPLC; column: Lux[®] Amylose-1 (250 × 4.6 mm i.d., 5 μ m), Mobile phase: *n*-hexane:ethanol (70:30 *v/v*), 0.5 mL/min, λ_{max} 254 nm).

(*R*)-1-((1-Hydroxypropan-2-yl)amino)-4-propoxy-9H-thioxanthen-9-one (ATx 2 (-)). Yield: 5.91%. m.p.: 118–120 °C (dec.); $[\alpha]_{\text{D}}^{25} -112^{\circ}$ ($c = 3.4 \times 10^{-3}$ g/mL in dichloromethane). IR (KBr) ν_{max} : 3447, 3282, 2963, 2927, 2874, 1611, 1595, 1569, 1506, 1436, 1290, 1270, 1252, 1226, 1072, 795, 746 cm⁻¹. ¹H-NMR (300.13 MHz, CDCl₃): δ : 8.50 (1H, d, $J = 8.1$ Hz, H-8), δ : 7.56 (2H, m, H-5 and H-6), δ : 7.42 (1H, m, H-7), δ : 7.13 (1H, d, $J = 9.1$ Hz, H-3), δ : 6.82 (1H, d, $J = 9.1$ Hz, H-2), δ : 4.04 (2H, t, $J = 6.5$ Hz, H-a), δ : 3.78 (3H, m, H-1' and CH₂OH), δ : 1.90 (2H, m, H-b), δ : 1.33 (3H, d, $J = 6.3$ Hz, H-2'), δ : 1.11 (3H, m, H-c). ¹³C-NMR (75.47 MHz, CDCl₃): δ : 183.56 (C-9), 146.80 (C-4), 144.00 (C-1), 136.82 (C-6), 131.87 (C-8a), 129.91 (C-4a), 129.22 (C-9a), 126.05 (C-8), 125.97 (C-7), 125.20 (C-5), 119.35 (C-3), 114.00 (C-10a), 109.02 (C-2), 72.52 (C-a), 66.04 (C-CH₂OH), 51.55 (C-1'), 22.70 (C-b), 17.00 (C-2'), 10.71 (C-c). e.e. > 99% (HPLC; column: Lux[®] Amylose-1 (250 × 4.6 mm i.d., 5 μ m), Mobile phase: *n*-hexane:ethanol (70:30 *v/v*), 0.5 mL/min, λ_{max} 254 nm).

(*S*)-1-((2-Hydroxypropyl)amino)-4-propoxy-9H-thioxanthen-9-one (ATx 3 (+)). Yield: 7.86%. m.p.: 149–152 °C (dec.); $[\alpha]_{\text{D}}^{25} -12^{\circ}$ ($c = 6.67 \times 10^{-3}$ g/mL in dichloromethane). IR (KBr) ν_{max} : 3460, 3320, 2965, 2933, 2875, 1607, 1566, 1556, 1502, 1450, 1434, 1286, 1269, 1249, 1227, 1158, 1133, 1060, 744 cm⁻¹. ¹H-NMR (300.13 MHz, CDCl₃): δ : 8.52 (1H, d, $J = 8.1$ Hz, H-8), δ : 7.56 (2H, m, H-5 and H-6), δ : 7.42 (1H, m, H-7), δ : 7.13 (1H, d, $J = 9.0$ Hz, H-3), δ : 6.78 (1H, d, $J = 9.0$ Hz, H-2), δ : 4.26 (1H, m, H-2'), δ : 4.03 (2H, t, $J = 6.5$ Hz, H-a), δ : 3.30 (2H, m, H-1'), δ : 1.90 (2H, m, H-b), δ : 1.35 (3H, d, $J = 6.3$ Hz, CH₃), δ : 1.12 (3H, t, $J = 7.4$ Hz, H-c). ¹³C-NMR (75.47 MHz, CDCl₃): δ : 183.46 (C-9), 146.18 (C-4), 144.01 (C-1), 136.98 (C-6), 133.27 (C-8a), 129.54 (C-4a), 129.43 (C-9a), 127.19 (C-8), 126.32 (C-7), 126.10 (C-5), 117.94

(C-3), 115.36 (C-10a), 111.83 (C-2), 72.31 (C-a), 65.58 (C-2'), 54.12 (C-1'), 22.74 (C-b), 20.97 (C-CH₃), 14.15 (C-c). e.e. > 99% (HPLC; column: Lux[®] Amylose-1 (250 × 4.6 mm i.d., 5 μm), Mobile phase: methanol, 0.5 mL/min, λ_{max} 254 nm).

(R)-1-((2-Hydroxypropyl)amino)-4-propoxy-9H-thioxanthen-9-one (ATx 4 (-)). Yield: 23.62%. m.p.: 145–150 °C (dec.); [α]_D²⁵ +12° (c = 6.67 × 10⁻³ g/mL in dichloromethane). IR (KBr) ν_{max}: 3460, 3323, 2966, 2932, 2875, 1606, 1566, 1556, 1501, 1451, 1434, 1328, 1286, 1270, 1249, 1227, 1158, 1133, 1102, 1060, 972, 744 cm⁻¹. ¹H-NMR (300.13 MHz, CDCl₃): δ: 8.51 (1H, d, J = 8.0 Hz, H-8), δ: 7.50 (2H, m, H-5 and H-6), δ: 7.41 (1H, m, H-7), δ: 7.12 (1H, d, J = 9.0 Hz, H-3), δ: 6.73 (1H, d, J = 9.0 Hz, H-2), δ: 4.22 (1H, m, H-2'), δ: 4.03 (2H, t, J = 6.4 Hz, H-a), δ: 3.29 (2H, m, H-1'), δ: 1.90 (2H, m, H-b), δ: 1.35 (3H, d, J = 6.3, CH₃), δ: 1.12 (3H, t, J = 7.4, H-c). ¹³C-NMR (75.47 MHz, CDCl₃): δ: 183.46 (C-9), 147.48 (C-4), 143.91 (C-1), 136.81 (C-6), 131.83 (C-8a), 129.92 (C-4a), 129.85 (C-9a), 129.26 (C-8), 126.02 (C-7), 125.95 (C-5), 119.25 (C-3), 113.95 (C-10a), 108.42 (C-2), 72.47 (C-a), 66.11 (C-2'), 52.07 (C-1'), 22.85 (C-b), 21.02 (C-CH₃), 10.71 (C-c). e.e. > 99% (HPLC; column: Lux[®] Amylose-1 (250 × 4.6 mm i.d., 5 μm), Mobile phase: methanol, 0.5 mL/min, λ_{max} 254 nm).

(S)-1-((1-Hydroxy-4-methylpentan-2-yl)amino)-4-propoxy-9H-thioxanthen-9-one (ATx 5 (+)). Yield: 19.59%. m.p.: 82–85 °C (dec.); [α]_D²⁵ -68° (c = 6.75 × 10⁻³ g/mL in dichloromethane). IR (KBr) ν_{max}: 3457, 3290, 2955, 2923, 2870, 1613, 1595, 1566, 1505, 1464, 1435, 1386, 1265, 1224, 1107, 1067, 1018, 745 cm⁻¹. ¹H-NMR (300.13 MHz, CDCl₃): δ: 8.51 (1H, d, J = 8.1 Hz, H-8), δ: 7.57 (2H, m, H-5 and H-6), δ: 7.42 (1H, m, H-7), δ: 7.13 (1H, d, J = 9.0 Hz, H-3), δ: 6.93 (1H, d, J = 9.0 Hz, H-2), δ: 4.04 (2H, t, J = 6.5 Hz, H-a), δ: 3.88 (1H, dd, J = 10.1 Hz, H-1'), δ: 3.71 (2H, m, CH₂OH), δ: 1.85 (4H, m, H-b), δ: 1.78 (1H, m, H-3'), δ: 1.57 (1H, t, J = 6.9 Hz, H-2'), δ: 1.12 (3H, t, J = 7.4 Hz, H-c), δ: 0.94 (3H, d, J = 6.5 Hz, H-4'a), δ: 0.89 (3H, d, J = 6.5 Hz, H-4'b). ¹³C-NMR (75.47 MHz, CDCl₃): δ: 183.61 (C-9), 145.00 (C-4), 142.80 (C-1), 136.7 (C-6), 131.98 (C-8a), 129.97 (C-4a), 129.83 (C-9a), 129.28 (C-8), 126.11 (C-7), 126.00 (C-5), 119.05 (C-3), 114.43 (C-10a), 111.02 (C-2), 72.45 (C-a), 64.62 (C-1'), 55.01 (C-CH₂OH), 40.44 (C-2'), 24.90 (C-3'), 22.86 (C-4'a), 22.83 (C-4'b), 22.61 (C-b), 10.71 (C-c). e.e. > 99% (HPLC; column: Lux[®] Amylose-1 (250 × 4.6 mm i.d., 5 μm), Mobile phase: acetonitrile, 0.5 mL/min, λ_{max} 254 nm).

(R)-1-((1-Hydroxy-4-methylpentan-2-yl)amino)-4-propoxy-9H-thioxanthen-9-one (ATx 6 (-)). Yield: 10.40%. m.p.: 80–82 °C (dec.); [α]_D²⁵ +56° (c = 6.75 × 10⁻³ g/mL in dichloromethane). IR (KBr) ν_{max}: 3459, 3291, 2954, 2925, 2871, 1613, 1595, 1566, 1505, 1480, 1435, 1386, 1266, 1224, 1108, 1072, 1018, 746 cm⁻¹. ¹H-NMR (300.13 MHz, CDCl₃): δ: 8.51 (1H, d, J = 8.1 Hz, H-8), δ: 7.55 (2H, m, H-5 and H-6), δ: 7.42 (1H, m, H-7), δ: 7.12 (1H, d, J = 9.1 Hz, H-3), δ: 6.86 (1H, d, J = 9.1 Hz, H-2), δ: 4.03 (2H, t, J = 6.5 Hz, H-a), δ: 3.85 (1H, dd, J = 10.5, H-1'), δ: 3.72 (2H, m, CH₂OH), δ: 1.83 (4H, m, H-b), δ: 1.76 (1H, m, H-3'), δ: 1.57 (1H, t, J = 6.9 Hz, H-3'), δ: 1.12 (3H, t, J = 7.4 Hz, H-c), δ: 0.96 (3H, d, J = 6.5 Hz, H-4'a), δ: 0.89 (3H, d, J = 6.5 Hz, H-4'b). ¹³C-NMR (75.47 MHz, CDCl₃): δ: 183.61 (C-9), 145.00 (C-4), 142.80 (C-1), 136.82 (C-6), 131.87 (C-8a), 129.93 (C-4a), 129.24 (C-9a), 128.80 (C-8), 126.03 (C-7), 125.97 (C-5), 119.42 (C-3), 113.94 (C-10a), 108.80 (C-2), 72.49 (C-a), 64.87 (C-1'), 40.71 (C-2'), 24.92 (C-3'), 22.96 (C-4'a), 22.86 (C-4'b), 22.55 (C-b), 10.71 (C-c). e.e. > 99% (HPLC; column: Lux[®] Amylose-1 (250 × 4.6 mm i.d., 5 μm), Mobile phase: acetonitrile, 0.5 mL/min, λ_{max} 254 nm).

(S)-1-((1-Hydroxy-3-methylbutan-2-yl)amino)-4-propoxy-9H-thioxanthen-9-one (ATx 7 (+)). Yield: 10.12%. m.p.: 98–102 °C (dec.); [α]_D²⁵ -26° (c = 6.80 × 10⁻³ g/mL in dichloromethane). IR (KBr) ν_{max}: 3385, 3256, 2960, 2926, 2873, 2360, 1614, 1569, 1514, 1463, 1434, 1386, 1329, 1267, 1249, 1225, 1165, 1070, 1021, 744 cm⁻¹. ¹H-NMR (300.13 MHz, CDCl₃): δ: 8.54 (1H, d, J = 8.0 Hz, H-8), δ: 7.59 (2H, m, H-5 and H-6), δ: 7.45 (1H, m, H-7), δ: 7.14 (1H, d, J = 9.1 Hz, H-3), δ: 7.07 (1H, d, J = 9.1 Hz, H-2), δ: 4.06 (2H, t, J = 6.4 Hz, H-a), δ: 3.86 (2H, m, CH₂OH), δ: 3.53 (1H, m, H-1'), δ: 2.08 (1H, m, H-2'), δ: 1.91 (2H, m, H-b), δ: 1.05 (3H, d, J = 6.9 Hz, H-3'a), δ: 0.87 (3H, d, J = 6.9 Hz, H-3'b), δ: 1.12 (3H, t, m, H-c). ¹³C-NMR (75.47 MHz, CDCl₃): δ: 183.43 (C-9), 145.0 (C-4), 142.8 (C-1), 136.43 (C-6), 131.66 (C-8a), 129.53 (C-4a), 129.03 (C-9a), 128.84 (C-8), 125.70 (C-7), 125.51 (C-5), 117.82 (C-3), 114.71 (C-10a), 111.6 (C-2), 71.80 (C-a), 63.93 (C-1'), 61.56 (C-CH₂OH), 29.15 (C-2'), 22.21 (C-b), 18.53 (C-3'a), 18.41 (C-3'b), 10.14 (C-c).

e.e. > 99% (HPLC; column: Lux[®] Amylose-1 (250 × 4.6 mm i.d., 5 μm), Mobile phase: acetonitrile, 0.5 mL/min, λ_{max} 254 nm).

(*R*)-1-((1-Hydroxy-3-methylbutan-2-yl)amino)-4-propoxy-9H-thioxanthen-9-one (ATx 8 (–)). Yield: 10.24%. m.p.: 98–104 °C (dec.); [α]_D²⁵ +26° (c = 6.80 × 10^{−3} g/mL in dichloromethane). IR (KBr) ν_{max}: 3423, 3272, 2959, 2925, 2872, 1611, 1570, 1511, 1463, 1435, 1385, 1251, 1226, 1161, 1068, 1022, 747 cm^{−1}. ¹H-NMR(300.13 MHz, CDCl₃): δ: 8.56 (1H, d, J = 8.0 Hz, H-8), δ: 7.64 (2H, m, H-5 and H-6), δ: 7.49 (1H, m, H-7), δ: 7.34 (1H, d, J = 8.9 Hz, H-3), δ: 7.17 (1H, d, J = 8.9 Hz, H-2), δ: 4.10 (2H, t, J = 6.4 Hz, H-a), δ: 3.90 (2H, m, CH₂OH), δ: 3.50 (1H, m, H-1'), δ: 2.10 (1H, m, H-2'), δ: 1.91 (2H, m, H-b), δ: 1.02 (3H, d, J = 6.9 Hz, H-3'a), δ: 0.98 (3H, d, J = 6.9 Hz, H-3'b), δ: 1.14 (3H, t, m, H-c); ¹³C-NMR (75.47 MHz, CDCl₃): δ: 183.65 (C-9), 147.74 (C-4), 141.53 (C-1), 137.16 (C-6), 132.60 (C-8a), 130.43 (C-4a), 129.52 (C-9a), 129.21 (C-8), 126.52 (C-7), 126.19 (C-5), 117.12 (C-3), 116.69 (C-10a), 115.38 (C-2), 72.19 (C-a), 67.02 (C-1'), 61.17 (CH₂OH), 28.87 (C-2'), 22.65 (C-b), 19.31 (C-3'a), 18.58 (C-3'b), 10.69 (C-c). e.e. > 99% (HPLC; column: Lux[®] Amylose-1 (250 × 4.6 mm i.d., 5 μm), Mobile phase: acetonitrile, 0.5 mL/min, λ_{max} 254 nm).

4.3. Caco-2 Cell Culture

For the *in vitro* assays, the Caco-2 cell model was used, which derived from human colorectal adenocarcinoma. The cells were routinely cultured in 75 cm² flasks and maintained in a 5% CO₂–95% air atmosphere, at 37 °C. Dulbecco's modified Eagle's medium (DMEM) supplemented with 10% heat-inactivated fetal bovine serum (FBS), 100 μM nonessential amino acids (NEAA), 100 U/mL penicillin, 100 μg/mL streptomycin and 6 μg/mL transferrin was used and changed every 2 to 3 days. Cultures were passaged weekly by trypsinization (0.25% trypsin/1 mM EDTA). For all the experiments, the cells were taken between the 27th and 36th passages. The cells were always seeded at a density of 60,000 cells/cm² and used 3 days after seeding, when confluence was reached. For the cytotoxicity assays the cells were seeded in 96-well plates, while for the evaluation of P-gp expression and P-gp transport activity, the cells were seeded in 12-well plates.

4.4. Compounds Cytotoxicity Assays

The cytotoxicity of the chiral ATxs 1–8 (0–50 μM) was accessed by the NR uptake assay, 24 h after exposure. The NR uptake assay provides a quantitative estimation of the number of viable cells in a culture based on the ability of viable cells to incorporate and bind the supravital dye NR in the lysosomes [30]. For that purpose, the cells were seeded onto 96-well plates and exposed to the eight tested ATxs 1–8 (0–50 μM) in fresh cell culture medium. After a 24 h incubation period, the cells were incubated with NR (40 μg/mL in cell culture medium) at 37 °C, in a humidified, 5% CO₂–95% air atmosphere, for 60 min. The cell culture was then removed, the dye absorbed only by viable cells extracted (with absolute ethyl alcohol/distilled water (1:1 *v/v*) containing 5% acetic acid) and the absorbance measured at 540 nm in a multiwell plate reader (BioTek Synergy[™] HT, BioTek, Winooski, VT, USA). At least five independent experiments were performed, in triplicate, and the percentage of NR uptake relative to that of the control cells was used as the cytotoxicity measure.

4.5. Flow Cytometry Analysis of P-gp Expression

P-gp expression was evaluated by flow cytometry using a P-gp monoclonal antibody [UIC2] conjugated with phycoerythrin (PE) [30]. For that purpose, Caco-2 cells were seeded onto 12-well plates, and exposed, three days after seeding, to the eight tested ATxs 1–8 (20 μM) in fresh cell culture medium. After 24 h of incubation, the cells were washed with HBSS buffer and harvested by trypsinization (0.25% trypsin/1 mM EDTA) to obtain a cellular suspension. After centrifugation (300× *g*, for 10 min, at 4 °C), the cells were suspended in HBSS buffer containing the P-gp antibody, being the antibody dilution selected accordingly to the manufacturer's instructions for flow cytometry. After a 30 min incubation, at 37 °C in the dark, with the UIC2 antibody, the cells were washed twice

with HBSS containing 10% heat-inactivated FBS, centrifuged ($300\times g$ for 10 min), suspended in ice-cold HBSS buffer and kept on ice until analysis. The fluorescence measurements of isolated cells were performed with a flow cytometer (BD Accuri™ C6, BD Biosciences, San Jose, California, USA), being the fluorescence of the UIC2-PE antibody measured by a 585 ± 40 nm band-pass filter (FL2). The logarithmic fluorescence was recorded and displayed as a single parameter histogram, and based on the acquisition of data for 20,000 cells. The parameter used for comparison was the mean of fluorescence intensity (MFI) [calculated as percentage of control ($0 \mu\text{M}$)]. In order to detect a possible contribution from cells autofluorescence to the analyzed fluorescence signals, non-labelled cells (with or without chiral thioxanthenes) were also analyzed in each experiment by a 585 ± 40 nm band-pass filter (FL2). Five independent experiments were performed in duplicate.

4.6. Evaluation of P-gp Transport Activity

The effect of the tested compounds on P-gp transport activity was accessed by flow cytometry using RHO 123 ($2 \mu\text{M}$) as a P-gp fluorescent substrate. Two different approaches were tested: a RHO 123 accumulation assay in the presence (IA) and absence (NA) of elacridar ($10 \mu\text{M}$), a known P-gp inhibitor, and with or without simultaneous exposure to ATxs 1–8 ($20 \mu\text{M}$) only during the RHO 123 accumulation phase; a RHO 123 accumulation assay, in the presence or absence of elacridar ($10 \mu\text{M}$), with or without pre-exposure of Caco-2 cells to ATxs 1–8 ($20 \mu\text{M}$) for 24 h.

4.6.1. RHO 123 Efflux Assay in the Presence of ATxs 1–8

For this purpose, the cells were seeded onto 75 cm^2 flasks and, after reaching confluence, harvested by trypsinization to obtain a cellular suspension, which was then divided into several aliquots of 300,000 cells. After centrifugation ($300\times g$ for 10 min), the cells were suspended in HBSS containing 10% heat-inactivated FBS and $2 \mu\text{M}$ RHO 123, with and without $20 \mu\text{M}$ ATxs 1–8, and incubated at 37°C , for 60 min, in the presence and absence of elacridar ($10 \mu\text{M}$). The cells were then washed twice with ice-cold HBSS with 10% heat-inactivated FBS, centrifuged ($300\times g$ for 10 min at 4°C) and kept on ice until flow cytometry analysis. The fluorescence measurements of isolated cells were performed as described in the section “Evaluation of P-gp expression”, being the RHO 123 fluorescence measured by a 530 ± 15 nm band-pass filter (FL1). The activity of the efflux pump was accessed by the RHO 123 accumulation ratio (Equation (1)) and expressed as percentage of control cells ($0 \mu\text{M}$ ATxs):

$$\text{RHO 123 accumulation} = \frac{\text{MFI of RHO 123 accumulation under inhibition (IA)}}{\text{MFI of RHO 123 normal accumulation (NA)}} \quad (1)$$

P-gp activity was assessed by ratio between the amount of RHO 123 accumulated under P-gp inhibition (with $10 \mu\text{M}$ elacridar) and the amount of RHO 123 accumulated in the absence of the P-gp inhibitor.

An increase in P-gp activity results in an increased RHO 123 efflux from the cells, which results in a decrease in the intracellular fluorescence intensity (decreased intracellular RHO 123 content). Therefore, a higher RHO 123 accumulation ratio (Equation (1)) is a consequence of a smaller MFI NA, which results from a higher P-gp activity since the dye is being effluxed out of the cells during the accumulation phase. Five independent experiments were performed in triplicate.

4.6.2. RHO 123 Efflux Assay in Caco-2 Cells Pre-Expose to ATxs 1–8 for 24 h

Caco-2 cells, seeded onto 12-well plates, were exposed to chiral thioxanthenes ($20 \mu\text{M}$), in fresh cell culture medium, for 24 h, prior to the evaluation of P-gp activity. After exposure, the cells were harvested by trypsinization to obtain a cell suspension, being the cells of each well divided into two aliquots. One aliquot was submitted to a RHO 123 accumulation phase under inhibited conditions (RHO 123 accumulation performed in IA conditions) and the second aliquot was submitted to a RHO 123 accumulation phase performed under normal conditions (RHO 123 accumulation performed in

NA conditions). For IA accumulation, the cells were centrifuged ($300\times g$ for 10 min) and suspended in HBSS buffer (pH 7.4) containing 10% heat-inactivated FBS, 2 μM RHO 123 and the P-gp inhibitor elacridar (10.0 μM), while for the NA accumulation a similar incubation was performed but in the absence of the P-gp inhibitor. In both cases, the cells were incubated with the P-gp substrate at 37 °C for 60 min to allow RHO 123 accumulation. After this accumulation period, the cells were washed twice with ice-cold HBSS buffer containing 10% heat-inactivated FBS and suspended in ice-cold HBSS buffer immediately before analysis. The evaluation of RHO 123 intracellular content was performed as described in the “Flow cytometry analysis of P-gp expression” section, being the RHO 123 fluorescence measured by a 530 ± 15 nm band-pass filter (FL1). The results were calculated according to the ratio defined in Equation (1) and expressed as percentage of control cells. Four independent experiments were performed in duplicate.

4.7. Evaluation of P-gp ATPase Activity

The effects of the tested ATxs 1–8 on P-gp ATPase activity were evaluated in recombinant human P-gp-enriched membranes, using the luminescent Pgp-Glo™ Assay (Promega Corporation, Madison, WI, USA), according to the manufacturer’s instructions.

Briefly, recombinant human P-gp-enriched membranes (25 $\mu\text{g}/\text{well}$) were incubated with 20 μM chiral thioxanthenes or sodium vanadate at 100 μM (positive control for P-gp ATPase activity inhibition) or verapamil at 200 μM (positive control for P-gp ATPase activity stimulation) in assay buffer, and 5 mM MgATP, for exactly 60 min, at 37 °C. After incubation, the reaction was stopped and the remaining ATP detected in a multi-well plate reader (BioTek Synergy™ HT), after a 20 min signal-developing period at room temperature, as a luciferase-generated luminescent signal.

The decreased luminescence of the untreated (NT) incubations relative to Na_3VO_4 -treated incubations reflects the basal P-gp ATPase activity. The decreased luminescence of incubations performed with the positive control drug verapamil relative to Na_3VO_4 -treated reactions reflects verapamil-stimulated P-gp ATPase activity. The luminescence of the chiral thioxanthenes incubations relative to that of the Na_3VO_4 -treated reactions reflects the effect, if any, of that compounds on P-gp ATPase activity (i.e., a decrease in luminescence reflects a stimulated P-gp ATPase activity). Three independent experiments were performed in triplicate for this assay and the results expressed as mean \pm SEM.

4.8. Statistical Analysis

All statistical calculations were performed with the GraphPad Prism version 6.00 for Windows (GraphPad Software, San Diego, CA, USA). Normality of the data distribution was assessed by three different tests (KS normality test, D’Agostino & Pearson omnibus normality test and Shapiro-Wilk normality test). Data obtained from the thioxanthenes cytotoxicity assays are expressed as mean \pm SEM from at least five independent experiments (performed in triplicate) and the statistical comparisons were estimated using the nonparametric method of Kruskal–Wallis, followed by the Dunn’s post hoc test. Data from the P-gp expression assays are presented as mean \pm SEM from five independent experiments (performed in duplicate) and the statistical comparisons were made using One-way ANOVA, followed by the Tukey’s multiple comparisons test. Results from the P-gp transport activity assays performed in the presence of chiral thioxanthenes during the RHO 123 accumulation phase are presented as mean \pm SEM from five independent experiments (performed in triplicate) and the statistical comparisons were estimated using One-way ANOVA, followed by the Tukey’s multiple comparisons test. Results from the P-gp transport activity assays performed in cells pre-exposed to chiral thioxanthenes for 24 h are presented as mean \pm SEM from four independent experiments (performed in duplicate) and the statistical comparisons were estimated using One-way ANOVA, followed by the Tukey’s multiple comparisons test. Results from the P-gp ATPase activity is presented as mean \pm SEM from three independent experiments (performed in triplicate) and the statistical

comparisons were estimated using One-way ANOVA, followed by the Tukey's multiple comparisons test. In all cases, *p* values lower than 0.05 were considered significant.

5. Conclusions

Thioxanthone derivatives and, particularly, aminated thioxanthenes, have been characterized as P-gp modulators. Since the pharmacokinetics, efficacy and safety of drugs that are P-gp substrates depend on the level of expression and functionality of P-gp, and can be affected by the chirality of compounds, it is important to better understand the effect that this important property may have in P-gp modulation. Therefore, in order to accomplish the main aim of this study, four enantiomeric pairs of thioxanthenes were synthesized through a copper catalyzed Ullman asymmetric coupling reaction that provided the desired chiral thioxanthenes with an e.e. > 99%. The assays carried out for the evaluation of the biological activity of the tested chiral ATxs 1–8 demonstrated that these compounds have the ability to immediately increase P-gp activity without interfering with its levels of expression and, therefore, can be characterized as P-gp activators. Chiral thioxanthenes 2 (–) and 7 (+) demonstrated to be the most efficient P-gp activators, among all the thioxanthenes tested.

Comparing the results obtained with both enantiomers of each enantiomeric pair, no significant enantioselectivity was observed for the direct modulation of P-gp. Nevertheless, the introduction of a chiral center close to the thioxanthonic scaffold favored their activation effect. Differences were noted in what concerns the induction effect, which may be related to their mechanism of induction, which deserves to be further explored. However, it is well known that P-gp expression is regulated by multiple signaling pathways, each involving different molecular targets and transcription factors, making the elucidation of the induction mechanism underlying ATX2-mediated P-gp induction a complex task. One of the possible pathways involved in the transcriptional activation of the *MDR1* gene expression involves the activation of the pregnane X receptor (PXR) [4,66], and several anticancer compounds, plant extracts, cholesterol-lowering statins, rifampicin and HIV protease inhibitors were already reported as PXR ligands [67–72]. Therefore, the potential enantioselectivity in what concerns to PXR activation deserves to be explored in future studies.

Acknowledgments: This research was partially supported by the Strategic Funding UID/Multi/04423/2013 through national funds provided by FCT—Foundation for Science and Technology and European Regional Development Fund (ERDF), in the framework of the programme PT2020, the project PTDC/MAR-BIO/4694/2014 (reference POCI-01-0145-FEDER-016790; Project 3599—Promover a Produção Científica e Desenvolvimento Tecnológico e a Constituição de Redes Temáticas (3599-PPCDT)) as well as by the project INNOVMAR—Innovation and Sustainability in the Management and Exploitation of Marine Resources (reference NORTE-01-0145-FEDER-000035, within Research Line NOVELMAR), supported by North Portugal Regional Operational Programme (NORTE 2020), under the PORTUGAL 2020 Partnership Agreement, through the European Regional Development Fund (ERDF). The authors also thank Sara Cravo, Department of Chemistry, Laboratory of Organic and Pharmaceutical Chemistry, Faculty of Pharmacy, University of Porto, for technical support in chiral HPLC. Renata Silva acknowledges Fundação para a Ciência e a Tecnologia (FCT) for her Post-doctoral grant (SFRH/BPD/110201/2015).

Author Contributions: E.S. and R.S. conceived the study design. A.L. synthesized the compounds and elucidated their structure and, C.F., E.S., and M.M.M.P. analyzed the data. A.L. performed the HPLC analysis and C.F. analyzed the data. A.L. and E.M. performed the cytotoxicity and P-gp assays, and R.S. and F.R. analyzed the data. A.L. and E.S. wrote the manuscript, while all authors gave significant contributions in discussion and revision.

Conflicts of Interest: The authors declare no conflict of interest. The founding sponsors had no role in the design of the study; in the collection, analyses, or interpretation of data; in the writing of the manuscript, and in the decision to publish the results.

References

1. Capparelli, E.; Zinzi, L.; Cantore, M.; Contino, M.; Perrone, M.G.; Luurtsema, G.; Berardi, F.; Perrone, R.; Colabufo, N.A. *Sar* studies on tetrahydroisoquinoline derivatives: The role of flexibility and bioisosterism to raise potency and selectivity toward P-glycoprotein. *J. Med. Chem.* **2014**, *57*, 9983–9994. [[CrossRef](#)] [[PubMed](#)]

2. Thiebaut, F.; Tsuruo, T.; Hamada, H.; Gottesman, M.M.; Pastan, I.; Willingham, M.C. Cellular localization of the multidrug-resistance gene product P-glycoprotein in normal human tissues. *Proc. Natl. Acad. Sci. USA* **1987**, *84*, 7735–7738. [[CrossRef](#)] [[PubMed](#)]
3. Varma, M.V.S.; Ashokraj, Y.; Dey, C.S.; Panchagnula, R. P-Glycoprotein inhibitors and their screening: A perspective from bioavailability enhancement. *Pharmacol. Res.* **2003**, *48*, 347–359. [[CrossRef](#)]
4. Silva, R.; Vilas-Boas, V.; Carmo, H.; Dinis-Oliveira, R.J.; Carvalho, F.; de Lourdes Bastos, M.; Remião, F. Modulation of P-glycoprotein efflux pump: Induction and activation as a therapeutic strategy. *Pharmacol. Ther.* **2015**, *149*, 1–123. [[CrossRef](#)] [[PubMed](#)]
5. Hennessy, M.; Spiers, J.P. A primer on the mechanics of P-glycoprotein the multidrug transporter. *Pharmacol. Res.* **2007**, *55*, 1–15. [[CrossRef](#)] [[PubMed](#)]
6. Sharom, F.J. ABC multidrug transporters: Structure, function and role in chemoresistance. *Pharmacogenomics* **2008**, *9*, 105–127. [[CrossRef](#)] [[PubMed](#)]
7. Sharom, F.J. The P-glycoprotein multidrug transporter. *Essays Biochem.* **2011**, *50*, 161–178. [[CrossRef](#)] [[PubMed](#)]
8. Sharom, F.J. The P-glycoprotein multidrug transporter: Interactions with membrane lipids, and their modulation of activity. *Biochem. Soc. Trans.* **1997**, *25*, 1088–1096. [[CrossRef](#)] [[PubMed](#)]
9. Gameiro, M.; Silva, R.; Rocha-Pereira, C.; Carmo, H.; Carvalho, F.; Bastos, M.L.; Remião, F. Cellular models and in vitro assays for the screening of modulators of P-gp, MRP1 and BCRP. *Molecules* **2017**, *22*, 600. [[CrossRef](#)] [[PubMed](#)]
10. Ambudkar, S.V.; Dey, S.; Hrycyna, C.A.; Ramachandra, M.; Pastan, I.; Gottesman, M.M. Biochemical, cellular, and pharmacological aspects of the multidrug transporter. *Annu. Rev. Pharmacol. Toxicol.* **1999**, *39*, 361–398. [[CrossRef](#)] [[PubMed](#)]
11. Leslie, E.M.; Deeley, R.G.; Cole, S.P.C. Multidrug resistance proteins: Role of P-glycoprotein, MRP1, MRP2, and BCRP (ABCG2) in tissue defense. *Toxicol. Appl. Pharmacol.* **2005**, *204*, 216–237. [[CrossRef](#)] [[PubMed](#)]
12. Fojo, A.T.; Ueda, K.; Slamon, D.J.; Poplack, D.G.; Gottesman, M.M.; Pastan, I. Expression of a multidrug-resistance gene in human tumors and tissues. *Proc. Natl. Acad. Sci. USA* **1987**, *84*, 265–269. [[CrossRef](#)] [[PubMed](#)]
13. Kobori, T.; Harada, S.; Nakamoto, K.; Tokuyama, S. Mechanisms of P-glycoprotein alteration during anticancer treatment: Role in the pharmacokinetic and pharmacological effects of various substrate drugs. *J. Pharmacol. Sci.* **2014**, *125*, 242–254. [[CrossRef](#)] [[PubMed](#)]
14. DeGorter, M.K.; Xia, C.Q.; Yang, J.J.; Kim, R.B. Drug transporters in drug efficacy and toxicity. *Annu. Rev. Pharmacol. Toxicol.* **2012**, *52*, 249–273. [[CrossRef](#)] [[PubMed](#)]
15. Couture, L.; Nash, J.A.; Turgeon, J. The ATP-binding cassette transporters and their implication in drug disposition: A special look at the heart. *Pharmacol. Rev.* **2006**, *58*, 244–258. [[CrossRef](#)] [[PubMed](#)]
16. Estudante, M.; Morais, J.G.; Soveral, G.; Benet, L.Z. Intestinal drug transporters: An overview. *Adv. Drug Deliv. Rev.* **2013**, *65*, 1340–1356. [[CrossRef](#)] [[PubMed](#)]
17. Doring, B.; Petzinger, E. Phase 0 and phase iii transport in various organs: Combined concept of phases in xenobiotic transport and metabolism. *Drug Metab. Rev.* **2014**, *46*, 261–282. [[CrossRef](#)] [[PubMed](#)]
18. Zhou, S.F. Structure, function and regulation of P-glycoprotein and its clinical relevance in drug disposition. *Xenobiotica* **2008**, *38*, 802–832. [[CrossRef](#)] [[PubMed](#)]
19. Miller, D.S.; Bauer, B.; Hartz, A.M. Modulation of P-glycoprotein at the blood-brain barrier: Opportunities to improve central nervous system pharmacotherapy. *Pharmacol. Rev.* **2008**, *60*, 196–209. [[CrossRef](#)] [[PubMed](#)]
20. Limtrakul, P.; Chearwae, W.; Shukla, S.; Phisalpong, C.; Ambudkar, S.V. Modulation of function of three abc drug transporters, P-glycoprotein (ABCB1), mitoxantrone resistance protein (ABCG2) and multidrug resistance protein 1 (ABCC1) by tetrahydrocurcumin, a major metabolite of curcumin. *Mol. Cell. Biochem.* **2007**, *296*, 85–95. [[CrossRef](#)] [[PubMed](#)]
21. Juliano, R.L.; Ling, V. A surface glycoprotein modulating drug permeability in chinese hamster ovary cell mutants. *Biochim. Biophys. Acta* **1976**, *455*, 152–162. [[CrossRef](#)]
22. Krishna, R.; Mayer, L.D. Multidrug resistance (MDR) in cancer: Mechanisms, reversal using modulators of MDR and the role of MDR modulators in influencing the pharmacokinetics of anticancer drugs. *Eur. J. Pharm. Sci.* **2000**, *11*, 265–283. [[CrossRef](#)]
23. Coley, H.M. Overcoming multidrug resistance in cancer: Clinical studies of P-glycoprotein inhibitors. *Methods Mol. Biol.* **2010**, *596*, 341–358. [[PubMed](#)]

24. Choong, E.; Dobrin, M.; Carrupt, P.A.; Eap, C.B. The permeability P-glycoprotein: A focus on enantioselectivity and brain distribution. *Expert Opin. Drug Metab. Toxicol.* **2010**, *6*, 953–965. [[CrossRef](#)] [[PubMed](#)]
25. Palmeira, A.; Sousa, E.; Vasconcelos, M.H.; Pinto, M.M. Three decades of P-gp inhibitors: Skimming through several generations and scaffolds. *Curr. Med. Chem.* **2012**, *19*, 1946–2025. [[CrossRef](#)] [[PubMed](#)]
26. Bansal, T.; Jaggi, M.; Khar, R.K.; Talegaonkar, S. Emerging significance of flavonoids as P-glycoprotein inhibitors in cancer chemotherapy. *J. Pharm. Pharm. Sci.* **2009**, *12*, 46–78. [[CrossRef](#)] [[PubMed](#)]
27. Palmeira, A.; Rodrigues, F.; Sousa, E.; Pinto, M.; Vasconcelos, M.H.; Fernandes, M.X. New uses for old drugs: Pharmacophore-based screening for the discovery of P-glycoprotein inhibitors. *Chem. Biol. Drug Des.* **2011**, *78*, 57–72. [[CrossRef](#)] [[PubMed](#)]
28. McDevitt, C.A.; Callaghan, R. How can we best use structural information on P-glycoprotein to design inhibitors? *Pharm. Ther.* **2007**, *113*, 429–441. [[CrossRef](#)] [[PubMed](#)]
29. Wang, R.B.; Kuo, C.L.; Lien, L.L.; Lien, E.J. Structure-activity relationship: Analyses of P-glycoprotein substrates and inhibitors. *J. Clin. Pharm. Ther.* **2003**, *28*, 203–228. [[CrossRef](#)] [[PubMed](#)]
30. Silva, R.; Palmeira, A.; Carmo, H.; Barbosa, D.J.; Gameiro, M.; Gomes, A.; Paiva, A.M.; Sousa, E.; Pinto, M.; Bastos Mde, L.; et al. P-glycoprotein induction in caco-2 cells by newly synthesized thioxanones prevents paraquat cytotoxicity. *Arch. Toxicol.* **2015**, *89*, 1783–1800. [[CrossRef](#)] [[PubMed](#)]
31. Silva, R.; Carmo, H.; Dinis-Oliveira, R.; Cordeiro-da-Silva, A.; Lima, S.C.; Carvalho, F.; Bastos Mde, L.; Remiao, F. In vitro study of P-glycoprotein induction as an antidotal pathway to prevent cytotoxicity in caco-2 cells. *Arch. Toxicol.* **2011**, *85*, 315–326. [[CrossRef](#)] [[PubMed](#)]
32. Silva, R.; Sousa, E.; Carmo, H.; Palmeira, A.; Barbosa, D.J.; Gameiro, M.; Pinto, M.; Bastos Mde, L.; Remiao, F. Induction and activation of P-glycoprotein by dihydroxylated xanones protect against the cytotoxicity of the P-glycoprotein substrate paraquat. *Arch. Toxicol.* **2014**, *88*, 937–951. [[CrossRef](#)] [[PubMed](#)]
33. Vilas-Boas, V.; Silva, R.; Palmeira, A.; Sousa, E.; Ferreira, L.M.; Branco, P.S.; Carvalho, F.; Bastos Mde, L.; Remiao, F. Development of novel rifampicin-derived P-glycoprotein activators/inducers. Synthesis, in silico analysis and application in the rbe4 cell model, using paraquat as substrate. *PLoS ONE* **2013**, *8*, e74425. [[CrossRef](#)] [[PubMed](#)]
34. Mizuno, N.; Sugiyama, Y. Drug transporters: Their role and importance in the selection and development of new drugs. *Drug Metab. Pharm.* **2002**, *17*, 93–108. [[CrossRef](#)]
35. Rosi, D.; Peruzzotti, G.; Dennis, E.W.; Berberian, D.A.; Freele, H.; Archer, S. A new active metabolite of “Miracil D”. *Nature* **1965**, *208*, 1005–1006. [[CrossRef](#)] [[PubMed](#)]
36. Cioli, D.; Pica-Mattocchia, L.; Archer, S. Antischistosomal drugs: Past, present . . . and future? *Pharmacol. Ther.* **1995**, *68*, 35–85. [[CrossRef](#)]
37. Palmeira, A.; Vasconcelos, M.H.; Paiva, A.; Fernandes, M.X.; Pinto, M.; Sousa, E. Dual inhibitors of P-glycoprotein and tumor cell growth: (Re)discovering thioxanones. *Biochem. Pharmacol.* **2012**, *83*, 57–68. [[CrossRef](#)] [[PubMed](#)]
38. Bases, R.E.; Mendez, F. Topoisomerase inhibition by lucanthone, an adjuvant in radiation therapy. *Int. J. Radiat. Oncol. Biol. Phys.* **1997**, *37*, 1133–1137. [[CrossRef](#)]
39. Woo, S.; Kang, D.; Kim, J.; Lee, C.-S.; Lee, E.-S.; Jahng, Y.; Kwon, Y.; Na, Y. Synthesis, cytotoxicity and topoisomerase ii inhibition study of new thioxanone analogues. *Bull. Korean Chem. Soc.* **2008**, *29*, 471–474.
40. Kostakis, I.K.; Pouli, N.; Marakos, P.; Mikros, E.; Skaltsounis, A.-L.; Leonce, S.; Atassi, G.; Renard, P. Synthesis, cytotoxic activity, nmr study and stereochemical effects of some new pyrano[3,2-b]thioxanthen-6-ones and pyrano[2,3-c]thioxanthen-7-ones. *Bioorg. Med. Chem.* **2001**, *9*, 2793–2802. [[CrossRef](#)]
41. Chen, C.-L.; Chen, T.-C.; Lee, C.-C.; Shih, L.-C.; Lin, C.-Y.; Hsieh, Y.-Y.; Ali, A.A.A.; Huang, H.-S. Synthesis and evaluation of new 3-substituted-4-chloro-thioxanone derivatives as potent anti-breast cancer agents. *Arab. J. Chem.* **2015**. [[CrossRef](#)]
42. Palmeira, A.; Sousa, E.; Fernandes, M.X.; Pinto, M.M.; Vasconcelos, M.H. Multidrug resistance reversal effects of aminated thioxanones and interaction with cytochrome P450 3A4. *J. Pharm. Pharm. Sci.* **2012**, *15*, 31–45. [[CrossRef](#)] [[PubMed](#)]
43. Horwitz, J.P.; Massova, I.; Wiese, T.E.; Besler, B.H.; Corbett, T.H. Comparative molecular field analysis of the antitumor activity of 9h-thioxanthen-9-one derivatives against pancreatic ductal carcinoma 03. *J. Med. Chem.* **1994**, *37*, 781–786. [[CrossRef](#)] [[PubMed](#)]

44. Corbett, T.H.; Panchapor, C.; Polin, L.; Lowichik, N.; Pugh, S.; White, K.; Kushner, J.; Meyer, J.; Czarnecki, J.; Chinnukroh, S.; et al. Preclinical efficacy of thioxanthone SR271425 against transplanted solid tumors of mouse and human origin. *Investig. New Drugs* **1999**, *17*, 17–27. [[CrossRef](#)] [[PubMed](#)]
45. Varvaresou, A.; Tsoinias, A.; Papadaki-Valiraki, A.; Siatra-Papastaikoudi, T. New aza-thioxanthenes: Synthesis and cytotoxicity. *Bioorg. Med. Chem. Lett.* **1996**, *6*, 861–864. [[CrossRef](#)]
46. Neumann, M.G.; Gehlen, M.H.; Encinas, M.V.; Allen, N.S.; Corrales, T.; Peinado, C.; Catalina, F. Photophysics and photoreactivity of substituted thioxanthenes. *J. Chem. Soc. Faraday Trans.* **1997**, *93*, 1517–1521. [[CrossRef](#)]
47. Paiva, A.M.; Pinto, M.M.; Sousa, E. A century of thioxanthenes: Through synthesis and biological applications. *Curr. Med. Chem.* **2013**, *20*, 2438–2457. [[CrossRef](#)] [[PubMed](#)]
48. Belal, F.; Hefnawy, M.M.; Aly, F.A. Analysis of pharmaceutically-important thioxanthene derivatives. *J. Pharm. Biomed. Anal.* **1997**, *16*, 369–376. [[CrossRef](#)]
49. Lory, P.M.J.; Estrella-Jimenez, M.E.; Shashack, M.J.; Lokesh, G.L.; Natarajan, A.; Gilbertson, S.R. Synthesis and screening of 3-substituted thioxanthene-9-one-10,10-dioxides. *Bioorg. Med. Chem. Lett.* **2007**, *17*, 5940–5943. [[CrossRef](#)] [[PubMed](#)]
50. Chen, Z.; Shi, T.; Zhang, L.; Zhu, P.; Deng, M.; Huang, C.; Hu, T.; Jiang, L.; Li, J. Mammalian drug efflux transporters of the atp binding cassette (abc) family in multidrug resistance: A review of the past decade. *Cancer Lett.* **2016**, *370*, 153–164. [[CrossRef](#)] [[PubMed](#)]
51. Ferreira, A.; Pousinho, S.; Fortuna, A.; Falcão, A.; Alves, G. Flavonoid compounds as reversal agents of the P-glycoprotein-mediated multidrug resistance: Biology, chemistry and pharmacology. *Phytochem. Rev.* **2015**, *14*, 233–272. [[CrossRef](#)]
52. Silva, R.; Carmo, H.; Vilas-Boas, V.; de Pinho, P.G.; Dinis-Oliveira, R.J.; Carvalho, F.; Silva, I.; Correia-de-Sa, P.; Bastos Mde, L.; Remiao, F. Doxorubicin decreases paraquat accumulation and toxicity in caco-2 cells. *Toxicol. Lett.* **2013**, *217*, 34–41. [[CrossRef](#)] [[PubMed](#)]
53. Zhou, Q.; Yu, L.S.; Zeng, S. Stereoselectivity of chiral drug transport: A focus on enantiomer- transporter interaction. *Drug Metab. Rev.* **2014**, *46*, 283–290. [[CrossRef](#)] [[PubMed](#)]
54. Shen, S.; He, Y.; Zeng, S. Stereoselective regulation of mdr1 expression in caco-2 cells by cetirizine enantiomers. *Chirality* **2007**, *19*, 485–490. [[CrossRef](#)] [[PubMed](#)]
55. Pham, Y.-T.; Régina, A.; Farinotti, R.; Couraud, P.-O.; Wainer, I.W.; Roux, F.; Gimenez, F. Interactions of racemic mefloquine and its enantiomers with P-glycoprotein in an immortalised rat brain capillary endothelial cell line, GPNT. *Biochim. Biophys. Acta* **2000**, *1524*, 212–219. [[CrossRef](#)]
56. Sousa, M.E.; Tiritan, M.E.; Belaz, K.R.A.; Pedro, M.; Nascimento, M.S.J.; Cass, Q.B.; Pinto, M.M.M. Multimilligram enantioresolution of low-solubility xanthonolignoids on polysaccharide chiral stationary phases using a solid-phase injection system. *J. Chromatogr. A* **2006**, *1120*, 75–81. [[CrossRef](#)] [[PubMed](#)]
57. Fernandes, C.; Palmeira, A.; Ramos, I.; Carneiro, C.; Afonso, C.; Tiritan, M.; Cidade, H.; Pinto, P.; Saraiva, M.; Reis, S.; et al. Chiral derivatives of xanthenes: Investigation of the effect of enantioselectivity on inhibition of cyclooxygenases (COX-1 and COX-2) and binding interaction with human serum albumin. *Pharmaceuticals* **2017**, *10*, 50. [[CrossRef](#)] [[PubMed](#)]
58. Fernandes, C.; Masawang, K.; Tiritan, M.E.; Sousa, E.; Lima, V.; Afonso, C.; Bousbaa, H.; Sudprasert, W.; Pedro, M.; Pinto, M.M. New chiral derivatives of xanthenes: Synthesis and investigation of enantioselectivity as inhibitors of growth of human tumor cell lines. *Bioorg. Med. Chem.* **2014**, *22*, 1049–1062. [[CrossRef](#)] [[PubMed](#)]
59. Takara, K.; Hayashi, R.; Kokufu, M.; Yamamoto, K.; Kitada, N.; Ohnishi, N.; Yokoyama, T. Effects of nonsteroidal anti-inflammatory drugs on the expression and function of P-glycoprotein/mdr1 in caco-2 cells. *Drug Chem. Toxicol.* **2009**, *32*, 332–337. [[CrossRef](#)] [[PubMed](#)]
60. Silva, R.; Carmo, H.; Vilas-Boas, V.; Barbosa, D.J.; Palmeira, A.; Sousa, E.; Carvalho, F.; Bastos Mde, L.; Remiao, F. Colchicine effect on P-glycoprotein expression and activity: In silico and in vitro studies. *Chem. Biol. Interact.* **2014**, *218*, 50–62. [[CrossRef](#)] [[PubMed](#)]
61. Vilas-Boas, V.; Silva, R.; Gaio, A.R.; Martins, A.M.; Lima, S.C.; Cordeiro-da-Silva, A.; de Lourdes Bastos, M.; Remiao, F. P-Glycoprotein activity in human caucasian male lymphocytes does not follow its increased expression during aging. *Cytom. Part A J. Int. Soc. Anal. Cytol.* **2011**, *79*, 912–919. [[CrossRef](#)] [[PubMed](#)]

62. Taipalensuu, J.; Tornblom, H.; Lindberg, G.; Einarsson, C.; Sjoqvist, F.; Melhus, H.; Garberg, P.; Sjostrom, B.; Lundgren, B.; Artursson, P. Correlation of gene expression of ten drug efflux proteins of the atp-binding cassette transporter family in normal human jejunum and in human intestinal epithelial caco-2 cell monolayers. *J. Pharmacol. Exp. Ther.* **2001**, *299*, 164–170. [[PubMed](#)]
63. Chang, K.L.; Pee, H.N.; Yang, S.; Ho, P.C. Influence of drug transporters and stereoselectivity on the brain penetration of pioglitazone as a potential medicine against alzheimer's disease. *Sci. Rep.* **2015**, *5*, 9000. [[CrossRef](#)] [[PubMed](#)]
64. Zhu, C.-J.; Hua, F.; Zhu, X.-L.; Li, M.; Wang, H.-X.; Yu, X.-M.; Li, Y. Stereoselective regulation of P-gp activity by clausenamamide enantiomers in caco-2, kb/kbv and brain microvessel endothelial cells. *PLoS ONE* **2015**, *10*, e0135866. [[CrossRef](#)] [[PubMed](#)]
65. Smith, S.W. Chiral toxicology: It's the same thing...only different. *Toxicol. Sci.* **2009**, *110*, 4–30. [[CrossRef](#)] [[PubMed](#)]
66. Maglich, J.M.; Stoltz, C.M.; Goodwin, B.; Hawkins-Brown, D.; Moore, J.T.; Kliewer, S.A. Nuclear pregnane x receptor and constitutive androstane receptor regulate overlapping but distinct sets of genes involved in xenobiotic detoxification. *Mol. Pharmacol.* **2002**, *62*, 638–646. [[CrossRef](#)] [[PubMed](#)]
67. Chen, Y.; Tang, Y.; Guo, C.; Wang, J.; Boral, D.; Nie, D. Nuclear receptors in the multidrug resistance through the regulation of drug-metabolizing enzymes and drug transporters. *Biochem. Pharmacol.* **2012**, *83*, 1112–1126. [[CrossRef](#)] [[PubMed](#)]
68. Mani, S.; Huang, H.; Sundarababu, S.; Liu, W.; Kalpana, G.; Smith, A.B.; Horwitz, S.B. Activation of the steroid and xenobiotic receptor (human pregnane x receptor) by nontaxane microtubule-stabilizing agents. *Clin. Cancer Res.* **2005**, *11*, 6359–6369. [[CrossRef](#)] [[PubMed](#)]
69. Jacobs, M.N.; Nolan, G.T.; Hood, S.R. Lignans, bacteriocides and organochlorine compounds activate the human pregnane x receptor (PXR). *Toxicol. Appl. Pharmacol.* **2005**, *209*, 123–133. [[CrossRef](#)] [[PubMed](#)]
70. Synold, T.W.; Dussault, I.; Forman, B.M. The orphan nuclear receptor srx coordinately regulates drug metabolism and efflux. *Nat. Med.* **2001**, *7*, 584–590. [[CrossRef](#)] [[PubMed](#)]
71. Huang, R.; Murry, D.J.; Kolwankar, D.; Hall, S.D.; Foster, D.R. Vincristine transcriptional regulation of efflux drug transporters in carcinoma cell lines. *Biochem. Pharmacol.* **2006**, *71*, 1695–1704. [[CrossRef](#)] [[PubMed](#)]
72. Masuyama, H.; Suwaki, N.; Tateishi, Y.; Nakatsukasa, H.; Segawa, T.; Hiramatsu, Y. The pregnane X receptor regulates gene expression in a ligand- and promoter-selective fashion. *Mol. Endocrinol.* **2005**, *19*, 1170–1180. [[CrossRef](#)] [[PubMed](#)]

Sample Availability: Samples of the compounds ATxs 1–8 are available from the authors.



© 2018 by the authors. Licensee MDPI, Basel, Switzerland. This article is an open access article distributed under the terms and conditions of the Creative Commons Attribution (CC BY) license (<http://creativecommons.org/licenses/by/4.0/>).